# Design and Analysis of a Visible-Light-Communication Enhanced WiFi System

Sihua Shao, Abdallah Khreishah, Moussa Ayyash, Michael B. Rahaim, Hany Elgala, Volker Jungnickel, Dominic Schulz, Thomas D. C. Little, Jonas Hilt, and Ronald Freund

***Abstract*—Visible light communication (VLC) has wide unlicensed bandwidth, enables communication in radio-frequency-sensitive environments, realizes energy-efficient data transmission, and has the potential to boost the capacity of wireless access networks through spatial reuse. On the other hand, WiFi provides more coverage than VLC and does not suffer from the likelihood of blockage due to the line-of-sight requirement of VLC. In order to take the advantages of both WiFi and VLC, we propose and implement two heterogeneous systems with Internet access. One is the hybrid WiFi–VLC system, utilizing a unidirectional VLC channel as the downlink and reserving the WiFi backchannel as the uplink. The asymmetric solution resolves the optical uplink challenges and benefits from the full-duplex communication based on VLC. To further enhance the robustness and increase throughput, the other system is presented, in which we aggregate WiFi and VLC in parallel by leveraging the bonding technique in the Linux operating system. We also theoretically prove the superiority of the aggregated system in terms of average system delay. Online experiment results reveal that the hybrid system outperforms the conventional WiFi for crowded environments in terms of throughput and Web page loading time, and also demonstrate the further improved performance of the aggregated system when considering the blocking duration and the distance between the access point and the user device.**

***Index Terms*—Heterogeneous network (HetNet); Hybrid system; Link aggregation; Visible light communications (VLC); WiFi.**

## I. Introduction

The continuous growth in the adoption of mobile devices including smart phones, tablets, laptops, and now devices on the "Internet of Things" is driving an insatiable demand for data access to wireless networks. According to the Cisco Visual Networking Index [1], traffic from wireless and mobile devices will exceed the traffic from wired devices by 2019. By 2019, wired devices will account for 33% of IP traffic, while Wi-Fi and mobile devices will account for 66% of IP traffic. Although wireless providers are deploying additional access infrastructure by means of new cells and WiFi end points, the limitation is becoming overuse of the existing radio-frequency (RF) spectrum. This manifests as contention and interference, and results in an increase in latency and a decrease in network throughput—a "spectrum crunch" [2]. To alleviate this problem, new approaches to realize larger potential capacity at the wireless link are needed, and optical technologies including visible light communication (VLC) are excellent candidates.

VLC technology provided with LED devices is characterized by high area spectral efficiency, unlicensed wide bandwidth, high security, and dual-use nature [3]. For example, Fig. 1 shows how VLC can reuse spectrum efficiently in a small area. Case (a) shows a WiFi channel in which three users share a 30 Mb/s bandwidth, compared to case (b), a VLC-enabled environment, in which three users utilize individual 10 Mb/s VLC channels. Although the total bandwidth allocated to the three users is the same in the two cases, the outcome aggregated throughput of case (b) could be better than that of case (a), due to the contention effect on the RF channel, as we will see later. It is worth noticing that the gain of the VLC channel highly depends on the strict alignment between VLC transceivers. In contrast to the omnidirectional WiFi channel, the mobility of users will lead to severe degradation of VLC channel gain. Nevertheless, in this paper, the users' locations are assumed to be fixed, and the mobility issue is out of the scope of this paper. As a complementary approach to the existing wireless RF solutions, VLC is poised to overcome the crowded radio spectrum in highly localized systems and become a promising broadband wireless access candidate to resolve the "spectrum crunch."

LED-based indoor VLC has attracted great attention in recent years due to its innate physical properties including energy efficiency and lower operational cost compared to conventional incandescent and fluorescent lighting [4]. Current research on VLC focuses mainly on physical (PHY) layer techniques such as dimming support, flicker mitigation, and advanced modulation schemes [5]. These efforts seek to achieve the possible highest data rates. However, higher-level networking challenges must be addressed to enable interoperability in any practical network deployment [6–9].

Manuscript received February 18, 2015; revised June 24, 2015; accepted August 12, 2015; published September 10, 2015 (Doc. ID 234672).

S. Shao (e-mail: ss2536@njit.edu) and A. Khreishah are with the Department of Electrical and Computer Engineering, New Jersey Institute of Technology, Newark, New Jersey 07103, USA.

M. Ayyash is with the Department of Information Studies, Chicago State University, Chicago, Illinois 60628, USA.

M. B. Rahaim, H. Elgala, and T. D. C. Little are with the Department of Electrical and Computer Engineering, Boston University, Boston, Massachusetts 02215, USA.

V. Jungnickel, D. Schulz, J. Hilt, and R. Freund are with the Department of Photonic Networks and Systems, Fraunhofer-HHI, Berlin 10587, Germany.

http://dx.doi.org/10.1364/JOCN.7.000960

1943-0620/15/100960-14$15.00/0 

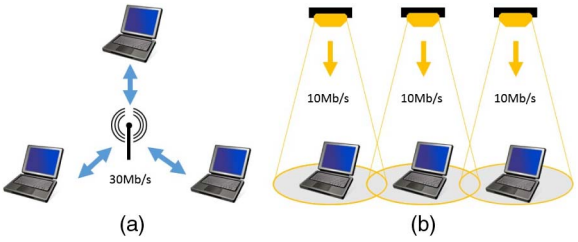


Fig. 1. Bandwidth density of (a) RF and (b) VLC.

Under a dual-use model, VLC is realized by overhead lighting—lights serve to provide lighting and also data access. However, providing an uplink in such a system is challenging due to the potential energy limitations of mobile devices (which do not need to produce light for illumination) and the potential glare from the produced light. In RF-sensitive and high-security applications, an optical uplink is possible with relatively high transmission speed [10]. However, in most RF-insensitive places such as homes, schools, offices, and supermarkets, an optical uplink is more difficult to justify. Mobile devices (e.g., laptops, smart phones, tablets) are energy-constrained. Equipping these devices with a power-hungry light source is impractical. To be efficient, VLC uplinks will need to use narrow beamwidths, which lead to challenges due to device motion and orientation with respect to fixed uplink receivers. Finally, VLC uplinks can produce glare that is uncomfortable to and undesirable for human users. Thus VLC remains a strong contender for the downlink channel but is better if complemented with an alternative uplink technology.

Alternative heterogeneous schemes, such as VLC and infrared [11], have been investigated by researchers in order to resolve the VLC uplink problem at the PHY layer. However, to make these approaches practical for networking, we still need to address challenges in realizing upper layer protocols when such an asymmetric model is adopted. Moreover, the ubiquitous nature of WiFi with its omnidirectional characteristic can be readily exploited as an uplink, especially if the use of VLC reduces congestion on the RF downlink.

In this paper, we propose and implement a practical hybrid system composed of typical IEEE 802.11 a/b/g/n technology and a VLC link, in which the unidirectional VLC channel is exploited to supplement the conventional downlink RF channel. Such a system was proposed and theoretically examined in [6]. Figure 2 shows the basic configuration of this heterogeneous network. Such a system not only alleviates congestion caused by WiFi access contention, but also resolves the potential problems of uplink transmission in VLC networking. For more information and also videos of experiments, please refer to our Web site.[1]

To further exploit the potential available resources of WiFi and VLC, we extend our investigation to the aggregation of multiple wireless interfaces. Although the hybrid

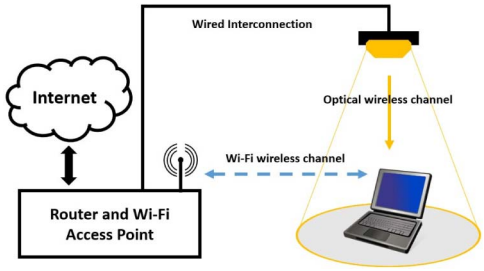


Fig. 2. Proposed hybrid WiFi and VLC network model.

solution alleviates congestion at the WiFi access point, the maximum achievable download data rate of this system is still limited by the single VLC link. In environments where VLC hotspots are deployed pervasively, we aim to utilize any available RF resources to supplement VLC links and provide additional capacity to devices requiring higher throughput. Referring to [12], we can benefit from the bandwidth aggregation for not only the improved throughput, but also the reliable packet delivery, load balancing, and low-cost capacity increase. It is also shown that many efforts have been spent on the bandwidth aggregation at different layers of the network protocol stack. Since our main objective is to implement the aggregation with modification to the clients only without affecting the server part, we focus our attention on data link layer aggregation.

In this paper, we utilize link aggregation through the use of two full-duplex wireless connections. Both the bidirectional WiFi and VLC links are fully utilized to improve the achievable throughput and provide more robust network connectivity. Figure 3 depicts the aggregated network. By combining multiple wireless access technologies, the system takes advantage of both communication techniques. We mathematically prove the superiority of the aggregated system with respect to the minimum average system delay. With optimal traffic allocation between WiFi and VLC, the aggregated system provides a lower minimum average system delay than another system that allocates each request to either WiFi or VLC.

The main contributions of the work are the following:

- The design and implementation of an asymmetric system composed of WiFi uplink and VLC downlink to increase the overall network capacity with multiple users.

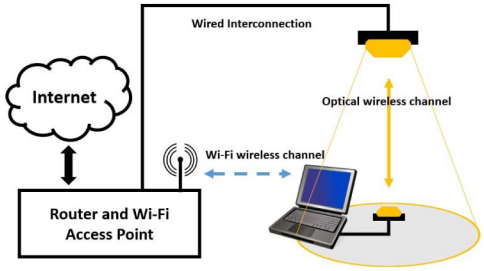


Fig. 3. Proposed aggregated WiFi and VLC network model.

[1]http://web.njit.edu/%7eabdallah/VLC/.

- The design and implementation of an aggregated system that simultaneously activates both WiFi and VLC connections providing high throughput and more reliable data transmission.
- Theoretical analysis that proves the superiority of the aggregated system over the nonaggregated system in terms of minimum average system delay.
- Analysis and real experimentation on our testbed to evaluate the network performance of two different systems under interactive Web browser traffic and TCP throughput with different levels of congestion.

The paper is organized as follows. Section II reviews related work on hybrid WiFi and VLC systems and data link layer aggregation. Section III describes the designed asymmetric system in detail including the router reconfiguration, packet capture, and retransmission—and, most significantly, the network-level operating system adaptations to realize the asymmetric protocols. We also demonstrate the detailed implementation of the aggregated system based on the bonding driver in the Linux operating system. In Section IV, we present two system models with and without aggregation. And we prove the superiority of the aggregated system in terms of average system delay. Section V provides analysis and experimental results demonstrating the benefit of the proposed hybrid and aggregated systems. Section VI concludes the paper.

## II. Related Work

Early work on hybrid systems integrating RF and VLC is based on simulation and analysis [6–9]. To the best of our knowledge, none of these hybrid systems were able to develop practical system implementations yielding functional IP-based communication supporting Web browsing or other Internet access functionalities.

A model for integrating WiFi and VLC has previously been proposed but not implemented [6]. In this model, downlink VLC channels are proposed to supplement an existing RF channel. Handover techniques are defined for resolving discontinuities due to mobility and specifically to transfer between a symmetric RF link and the asymmetric VLC–RF link as a device transits an indoor space. In this prior work, the primary contributions are simulation and analysis of the downlink channel under the assumption of a reliable RF uplink.

The device cost and energy consumption relative to data throughput have been investigated for a hybrid VLC system [7]. The authors show advantages for an RF uplink compared to a VLC uplink, but primarily as related to the energy cost for transmission. This work motivates us to study the hybrid system that replaces the energy-expensive uplink with RF.

Energy-efficient connectivity for hybrid radio-optical wireless systems has also been investigated in [8]. In this work the authors show via simulation that connectivity and energy consumption depend on the user device density, the coverage range ratio between single-hop and multi-hop, the relay probabilities, and the mobility of the user. Although the proposed WLAN–VLC network model shows the positive impact of a hybrid system, the approach they used relies on an ideal scenario that entails prior assumptions.

Room division multiplexing (RDM) has been demonstrated under a hybrid VLC network model [9]. The core component of this hybrid system is the VLC network coordinator, which is responsible for RDM-based service division and distribution as well as for providing bidirectional interfaces between the outdoor and indoor communication infrastructure, especially the indoor interfaces for uplink WiFi access and downlink LED lamps. This work, however, does not appear to extend to full implementation of the network protocol stack nor to implementation in the system kernel. Finally, the work is evaluated by waveform measurement without the signal processing and demodulation required for practical use.

Each of the aforementioned works focuses on simulation analysis without implementation of the full end-to-end system required to provide evaluation at the application layer. In contrast, we implement a practical hybrid WiFi–VLC wireless system, which enables the typical Internet access connection between client and server *without any reconfiguration at the server side*. Data packets generated by user applications are transmitted through WiFi, and requested data from the server is received via the VLC interface.

Early efforts on the data link layer aggregation were also based on the simulations [13–18]. To the best of our knowledge, none of the above work evaluates the performance of their presented policy based on real experiments.

The concept of a generic link layer (GLL) that aggregates multiple radio access at the radio level is introduced in [13]. The GLL enables multi-radio transmission diversity (MRTD), which transmits a traffic flow sequentially or parallel over aggregated radio access technologies. The significant functions in GLL include access selection schedule, performance monitoring, and flow error control. GLL blindly assigns the traffic to different interfaces. Based on the GLL concept, the authors further study the switched MRTD in [14]. Based on the measured throughput of each radio access technology, the work sorts the interfaces in descending order of their available throughput. The traffic flows are distributed to the interfaces in descending order. In Ref. [15], another factor, round trip time (RTT), is utilized to schedule the traffic through the interfaces. In Refs. [14] and [15], the switched MRTD is presented as an adaptive mode of the original MRTD. However, with similar available throughput over the interfaces, the proposed scheme produces inevitable redundant switching overheads.

A cognitive convergence layer (CCL), which is similar to GLL, is introduced in [16]. The authors propose a logic link layer interface for managing the traffic flows through real link layer interfaces. A traffic distribution policy is implemented at the sender, and a reorder buffer is added at the receiver. A function of link transmission time (LTT) is used to estimate the links' capacities. The CCL-based data link aggregation is further investigated in [17]. The authors use the link delay as a criterion to determine the data traffic

distribution over a tightly coupled WiMAX and WiFi network. In Ref. [18], the measurement of channel occupancy time for a single packet transmission is used as the decision metric. The air-time cost based scheme is reported as a more adaptive link aggregation schedule than the RTT-based policy.

All of the above-mentioned data link layer aggregation works focus on the network parameters, which are used for determining the link selection. None of them provided implementation of their proposed schemes or experimental analysis. In our work, we set up the testbed based on the bonding driver of Linux OS and evaluate the TCP throughput as well as the user experience for Web browsing. We also provide a rigorous mathematical analysis of our implemented system.

## III. System Model

In this section, we illustrate the models of two heterogeneous systems: 1) the hybrid WiFi–VLC system (Fig. 4) and 2) the aggregated WiFi–VLC system (Fig. 5).

### A. Hybrid System

**Challenges:** The primary challenges in designing an asymmetric system are as follows:

1) Typically, uplink and downlink data streams based on a WiFi connection between the client and the server flow through the same routing path. In order to redirect the data flow downloaded from the server to the client to the VLC hotspot, an intermediate coordinator is needed to break the conventional downlink data delivery and forward the data packets to the VLC hotspot. However, this process may generate inevitable redundancy due to the need for extra devices to perform data redirection. In Fig. 4, we aim to assign the infrastructural router as the redirecting node, forwarding downlink traffic to PC I and simultaneously providing PC II with uplink wireless access.
2) A typical small office home office (SOHO) wireless router has one wide area network (WAN) port and multiple local network (LAN) Ethernet ports. Terminals connected to the router through either wired or wireless links belong to the same subnetwork. This router serves as an edge router with a gateway IP address. Intuitively, we might be able to activate the routing function on PC I in Fig. 4, in order to directly forward the data packets from the router to PC II. However, due to the OS kernel built-redirecting function, the simple forwarding method based on the routing function may not be useful. Since the destination IP address of the data packets that arrive at the network interface card (NIC) A-1 is actually the IP address of NIC B-1, the packets will be redirected back to PC II through the router instead of the VLC link, if the forwarding function of PC I is activated.
3) In a typical TCP connection, the client initiates a three-phase handshake process with the server. According to the OSI model, the client first generates a SYN data segment at the application layer. After that, the data segment is encapsulated with IP headers at the network layer before being sent out through the NIC. Since the client starts listening to the socket with the same TCP port and IP address as that used during encapsulation, the following problem occurs. If the packets from the server are received from a different NIC with different socket information, they may not be selected by the application that initiated the TCP connection. In Fig. 4, the requests are transmitted through NIC B-1, while the responses are received from NIC B-2. The above problem is encountered in the asymmetric system in Fig. 4.

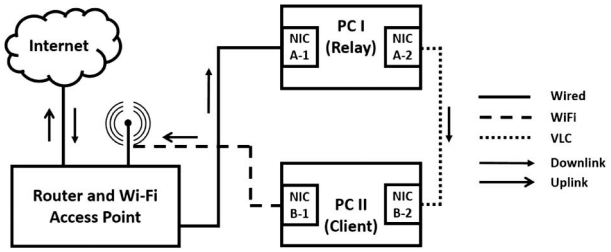


Fig. 4. Hybrid system architecture.

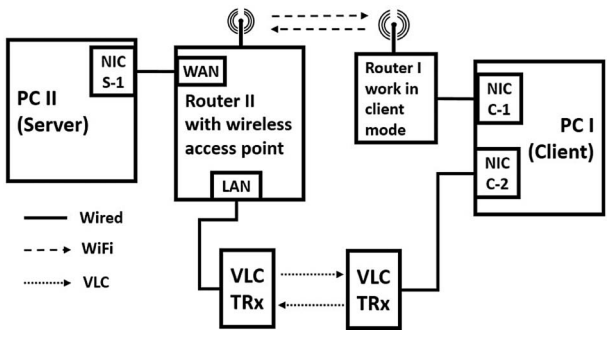


Fig. 5. Aggregated system architecture.

**System Design:** Figure 4 demonstrates the hybrid system model for indoor Internet access. The system consists of a downlink VLC channel and an uplink WiFi channel. To resolve the challenges mentioned earlier, three procedures (each one of these procedures corresponds to one of the above challenges) need to be performed as follows:

1) To address the problem mentioned in the first challenge, a static routing table is enabled at the router. Rather than dynamically forwarding IP packets as normal, the router follows a manually configured routing entry with three items: a) destination IP address, b) subnet mask, and c) next-hop router IP address. Table I shows an example of routing IP traffic destined for the 192.168.1.100/24 via the next-hop router with the IPv4 address of 192.168.1.200/24. In the

TABLE I
EXAMPLE OF STATIC ROUTING TABLE

| Dst IP | Subnet Mask | Next Hop | Metric |
|---|---|---|---|
| 192.168.1.100 | 255.255.255.255 | 192.168.1.200 | 2 |

proposed hybrid system, one active static routing rule redirects IP packets destined for NIC B-1 to NIC A-1 instead.

2) After successfully arriving at the relay node (PC I), server IP packets need to be further forwarded to the client through NIC A-2. In the Linux OS, the IP packet forwarding function is enabled by changing the value of *ip_forward* under the path "/proc/sys/net/ipv4/ip_forward" from 0 to 1. As mentioned in challenge 2 earlier, if we activate the forwarding function on PC I, the arrived IP packets will be redirected back to PC II through NIC A-1 instead of NIC A-2. Therefore, we must set the value of *ip_forward* to 0. Rather than relying on the forwarding function, we utilize the socket programming based on the SOCK_PACKET type [19].

   The SOCK_PACKET mechanism in Linux is used to take complete control of the Ethernet interfaces. Due to the capability of capturing frames from the data link layer and placing a pointer that points to the first byte of each frame (the first byte of the MAC header), SOCK_PACKET is suitable for MAC frame capturing and retransmission. Algorithm 1 represents the relaying functionality. In the algorithm, we first define the buffer size according to the maximum transmission unit (MTU), which is a default value in the router. Then two sockets of the SOCK_PACKET type are created and bound to NIC A-1 and NIC A-2. After the initialization phase of key parameters, the iteration phase, which includes receiving, processing, and retransmission, is started. To avoid the alert of no buffer space available for the sending function, the received frame length needs to be checked. If the length is larger than the defined MTU, the frame must be discarded. Also, the destination IP address of the captured frames for efficient relaying is checked. If it is the same as the IP address of NIC B-1, we manually modify the packet's MAC and destination IP address. To realize the Internet access, the checksums of IP, TCP, and UDP need to be recomputed before sending the packets to the client. This is because the checksum computation includes the destination IP address.

3) As mentioned in challenge (3) earlier, the application that initiates the TCP connection to the server will listen to the socket with the IP address of NIC B-1 but not of NIC B-2. The OS kernel will not perform any action on the packets although they are not filtered by the NIC. A possible solution is changing the destination IP of the packets to the IP address of NIC B-1. However, due to the fact that the destination IP address of the packets is not that of the port they are received from, the packets should be forwarded based on the routing table. To overcome this difficulty, an approach called "operating system spoofing" is proposed.

**Algorithm 1** Pseudo Code of Socket Program

```
Initialization:
  Define BufferSize MTU;
  Set socket s for frame capture;
  Set socket d for frame retransmission;
  Bind socket s to NIC A-1;
  Bind socket d to NIC A-2;
Iteration:
 1: while 1 do
 2:     Receive frames from socket s and store in buffer
        msg [BufferSize];
 3:     if frame length > MTU then
 4:       Continue;
 5:     end if
 6:     if frame desitination IP addr = IP B-1 then
 7:       Change dest MAC addr to MAC B-2;
 8:       Change src MAC addr to MAC A-2;
 9:       Change dest IP addr to IP B-2;
10:       Compute IP checksum;
11:       Compute TCP checksum;
12:       Compute UDP checksum;
13:       Send modified frames to socket d;
14:     end if
15: end while
```

*Operating System Spoofing:* The basic idea of this approach is to manually make the OS listen to NIC B-2 while transmitting out the packets through NIC B-1. Assume that the IP addresses of NIC B-2 is 192.168.2.100/24 and the default gateway of PC II is 192.168.1.1/24. The default gateway is deleted, and a new one within the subnet 192.168.2.0/24 (e.g., 192.168.2.1/24) is added. In addition, an entry in the ARP table on PC II (e.g., arp -s 192.168.2.1 ab:ab:ab:ab:ab:ab) is added. When these two steps are completed, PC II will believe that there is a next-hop gateway connected to NIC B-2 even though this gateway does not exist. With the ARP spoofing, all packets generated at the application layer on PC II are forwarded to NIC B-2 and stop there because of the physical layer blocking. The most significant point at this moment is that the applications are listening to the socket with the IP address of NIC B-2.

After the configuration of the routing and ARP tables, a socket program, which implements packet copying, header modification, and retransmission, is run. Similar to the program run on PC I, the socket of type SOCK_PACKET is used to capture the packets flowing through the device driver layer of NIC B-2. With the returned pointer, the source IP and MAC addresses of the copied packets to the IP and MAC addresses of NIC A-1 are altered. Also, we change the destination MAC address to the router's LAN MAC address. The checksums of IP, TCP, and UDP need to be recomputed. After all the modifications of the IP and MAC headers are completed, the packets are sent to the router through NIC B-1. From the router's point of view, the client's IP is the IP address of NIC B-1. However, from the client's point of view, it connects to the Internet with the IP address of NIC B-2. Figure 6 reveals the variation of IP and MAC headers.

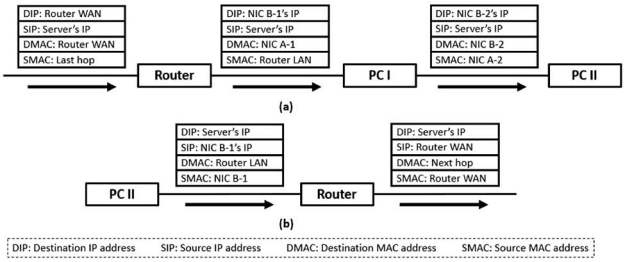


Fig. 6. Flow of MAC and IP headers of packets between server and client: (a) downlink flow and (b) uplink flow.

Note that, compared to the previously published work [20], the achievable network throughput of the proposed hybrid system has been enhanced [21]. For the packets captured on PC II, a selective condition before sending them to the router is added. Only the packets with a source IP the same as the IP address of NIC B-2 are processed by the program. Since the capture function returns the packets not only in the transmitting buffer of NIC B-2 but also in the receiving buffer, the added condition saves half of the redundant processing time in the unmodified program.

### *B. Aggregated System*

Figure 5 demonstrates the link aggregation system model including the full-duplex WiFi and VLC connections. Since the bonding driver provided by the Linux operating system is only capable of aggregating Ethernet interfaces, both NIC C-1 and NIC C-2 of PC I (client) are Ethernet cards. The wireless Router I working in client mode is connected to PC I through Ethernet cable and connected to Router II through a bidirectional WiFi link. The other network connection between PC I and Router II is a bidirectional VLC link, which is established by two VLC transceivers. The bidirectional VLC link will be described in Section V. The two NICs on PC I are in the same subnet, and the IP address of the Router II LAN is used as the IP address of the gateway of PC I, when the aggregation configuration is not enabled. On the right side, PC II (server) is connected to the WAN port of Router II.

To implement the data link layer aggregation, we utilize the Linux Ethernet bond driver [22]. The driver provides a method to aggregate multiple Ethernet interfaces into a single logical "bond" interface. The behavior of the artificial interface depends on the selected mode. There are seven modes in the bonding configuration: 0) Balance-rr, 1) Active-backup, 2) Balance-xor, 3) Broadcast, 4) 802.3ad, 5) Balance-tlb, and 6) Balance-alb. Modes 0, 2, and 4 require extra switch support, which conflicts with our objective of not having extra devices. Under Mode 1, only one slave in the bond is active. The other slave becomes active if and only if the active slave fails. Thus, the maximum throughput that can be achieved in this mode cannot exceed the highest one of the slaves. In Mode 3, the same packets are sent through all slave interfaces, in order to provide fault tolerance. Therefore, only Mode 5 and Mode 6 are left to choose from. For the goal of achieving higher aggregated throughput without any modification to the server side or even to the next hop of the client, Mode 6 is the best option.

Mode 6 (adaptive load balancing) contains Mode 5 (adaptive transmit load balancing). Also, Mode 6 integrates the receive load balancing for the IPv4 traffic and does not require any switch support. Load balancing at the receiver is achieved by ARP negotiation. The bond driver intercepts the ARP response sent from the host and changes the source MAC address to the unique MAC address of one of the slaves. It enables the peers to use a different MAC address for communication. Typically, all the slave ports will receive the broadcast ARP requests from the router. The bond driver module intercepts all the ARP responses sent from the client, and computes the corresponding port that the client expects to receive data from. Then the driver modifies the source MAC address of the ARP response to the MAC address of the corresponding port. The destination MAC address is kept the same as the MAC address of the router LAN. Note that each port can send the ARP response not only with its own MAC address but also with the MAC address of the other slave port. The received data traffic can be load balanced in either way. When the client sends the ARP request, the bonding driver copies and saves the IP information of the router. When the ARP reply from the router arrives, the bond driver extracts the MAC address of the router and sends an ARP response to one of the slave ports (this process is the same as the received load balancing process mentioned above). One potential problem in ARP negotiation is that when the client sends out the ARP request, it uses the MAC address of the logic bonding interface. Thus, after the router learns this MAC address, the downlink traffic from the server flows through the corresponding slave port, which may not be the intended one. This problem can be addressed by sending the updated ARP response. The client sends the ARP responses to all slave ports, and each response contains the unique MAC address of each slave port. Thus, the downlink traffic from the server is redistributed. The receive load [22] is allocated orderly from the slave with the widest bandwidth.

In Fig. 5, when Router II broadcasts an ARP request to PC I, PC I typically sends back an ARP response with the bonding MAC address and the bonding IP address. However, under adaptive load balancing mode, the bonding driver intercepts the APR response and changes the source MAC address to that of one of the slaves (e.g., NIC C-1). Thus, when the router receives the ARP response, it refreshes its ARP cache with a new entry (Bond IP: NIC C-1 MAC). To increase the total bandwidth of the client, PC I sends back the ARP response with the NIC C-2 MAC address when the capacity of NIC C-1 is exhausted. After receiving the new ARP response, the router updates its ARP cache (Bond IP: NIC C-2 MAC).

### *C. Analysis*

"Spectrum crunch" [2] is a challenging problem in WiFi networks. Due to the limited bandwidth, although the

efficiency of the spectrum utilization has been highly improved, the degradation of network throughput caused by the growing number of WiFi users and other devices operating in the 2.4 and 5 GHz bands is still inevitable. Also, the network delay could be much larger when the number of users in the same WiFi access point increases. Because of the CSMA/CA mechanism defined in 802.11 standards [23], the average back-off time is unavoidably increased when there exist more mobile users located in the same WiFi coverage. To circumvent these unexpected user experiences, the hybrid WiFi–VLC system is presented. Although the uplink WiFi may be in contention with other WiFi users, the downlink VLC is an independent data communication channel from the WiFi channels. In our daily life, downloading happens much more frequently than uploading; hence having an undisturbed VLC download channel may provide a satisfactory Internet surfing experience. Regarding the increasing demand for downlink bandwidth, the hybrid VLC user does not need to compete with other WiFi users for the RF spectrum. Therefore, the network delay will be reduced.

In some specific scenarios where uplink VLC is allowable, aggregating both bidirectional WiFi and VLC links can provide more available bandwidth. Taking the shortages of VLC into account, the aggregated system is more robust than the hybrid one. As the distance between the front-ends of WiFi and VLC is increasing or the channel blocking duration is increasing, the performance of the VLC channel may drop quickly. However, these two factors are not influential in WiFi communication when considering the short distance for indoor links. Aggregation may not only achieve higher average throughput, but also maintain the advantages of both WiFi and VLC.

## IV. System Delay Analysis

In this section, we show the benefits of the aggregated system theoretically. This is done by comparing the delay performance of this system to another system that assigns each request to either the VLC channel or the WiFi channel. In the aggregated system, any request is divided into two and the resulting two pieces of the request are forwarded to the WiFi and VLC channels, respectively. We also derive the optimal request splitting ratio. In the second system, the request is forwarded to either the WiFi or the VLC channel. The optimal ratios of the requests to be forwarded to either WiFi or VLC are also derived for this system. The major result we get in this section is that the minimum average delay of the aggregated system is always lower than that of the nonaggregated system. We realize that the effect of lower delay will be less drastic as the number of VLC hotspots increases. The objective of this theoretical analysis is to verify the superiority of the aggregated WiFi–VLC system over the nonaggregated one with respect to the optimal system delay and evaluate the degree of this superiority with different traffic patterns.

In our system model, we have one WiFi AP and one VLC hotspot. Requests arrive at the system according to a Poisson process with rate $\lambda$. The size of the request follows an exponential distribution with an average value of $\mu$. The bandwidths of the WiFi channel and the VLC channel are $B_1$ and $B_2$, respectively. We assume that $B_1 < B_2$.

### A. Aggregated System Analysis

Let $\alpha$ represent the percentage of the request's size that is sent to the WiFi channel. Based on the above discussion, the aggregated system can be represented by the queuing system in Fig. 7. Since one request is split into two and forwarded to each channel, the average request arrival rates for WiFi and VLC are both $\lambda$. Since $\mu$ represents the average request size, the average serving rates of WiFi and VLC are $B_1/\alpha\mu$ and $B_2/(1-\alpha)\mu$, respectively.

*Lemma 1:* In the aggregated system model, the minimum average system delay is $\frac{\mu}{B_1+B_2-\lambda\mu}$.

*Proof:* The optimization problem is written as follows:

$$\text{Objective: } \min E[\max(D_{\text{WiFi}}, D_{\text{VLC}})] \quad \text{s.t. } 0 \le \alpha \le 1,$$
$$\lambda < B_1/\alpha\mu, \quad \lambda < B_2/(1-\alpha)\mu, \quad B_1 < B_2. \tag{1}$$

Based on the M/M/1 queuing model, the average system delays of WiFi and VLC are exponentially distributed with average rates $D_{\text{WiFi}} = \frac{1}{[B_1/\alpha\mu]-\lambda}$ and $D_{\text{VLC}} = \frac{1}{[B_2/(1-\alpha)\mu]-\lambda}$, respectively. In the aggregated system model, when one request comes, it is separated into two. One part of the request is sent to the WiFi channel, and the other part is sent to the VLC channel at exactly the same time. Also the sizes of the two parts of the request are dependent. Therefore, minimizing the maximum delay of WiFi and VLC, given in Eq. (1), is equivalent to $D_{\text{WiFi}} = D_{\text{VLC}}$. According to the above discussion, we can conclude that the optimal $\alpha$ and the minimum average system delay are

$$\alpha_{\text{opt\_agg}} = \frac{B_1}{B_1+B_2},$$
$$D_{\text{min\_agg}} = \frac{\mu}{B_1+B_2-\lambda\mu}.$$

■

### B. Nonaggregated System Analysis

Let $\alpha$ denote the percentage of the requests that is sent to the WiFi channel. The nonaggregated system is equivalent to the queuing system in Fig. 8. We assume that the requests are randomly allocated to each channel. Hence, the request arrival for each queue is still a Poisson process.

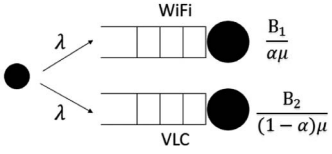


Fig. 7. Queuing model representing the aggregated system model.

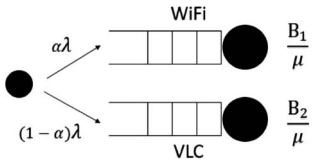


Fig. 8. Queuing model representing the nonaggregated system model.

The average request arrival rates in WiFi and VLC are $\alpha\lambda$ and $(1-\alpha)\lambda$, respectively. Since there is no request splitting in this model, the average serving rates of WiFi and VLC are $B_1/\mu$ and $B_2/\mu$, respectively.

*Lemma 2*: In the nonaggregated system model, the minimum average system delay is

$$D_{\text{min\_non\_agg}} = \begin{cases} \frac{2\lambda\mu - B_2\left(1-\sqrt{\beta}\right)^2}{\lambda[B_2(\beta+1)-\lambda\mu]}, & \text{if } \frac{B_2}{\lambda\mu}\left(1-\sqrt{\beta}\right) < 1 \\ \frac{\mu}{B_2-\lambda\mu}, & \text{otherwise} \end{cases}.$$

*Proof*: The optimization problem can be presented as follows:

$$\begin{aligned} \text{Objective: } & \min \alpha D_{\text{WiFi}} + (1-\alpha)D_{\text{VLC}} \\ & \text{s.t. } 0 \le \alpha \le 1, \\ & \alpha\lambda < B_1/\mu, \end{aligned} \tag{2}$$

$$(1-\alpha)\lambda < B_2/\mu, B_1 < B_2. \tag{3}$$

In order to find the candidate minimum point, we describe the average delay of the nonaggregated system as a function

$$\begin{aligned} D(\alpha) &= \alpha D_{\text{WiFi}} + (1-\alpha)D_{\text{VLC}} \\ &= \frac{\alpha}{B_1/\mu - \alpha\lambda} + \frac{1-\alpha}{B_2/\mu - (1-\alpha)\lambda}. \end{aligned}$$

We can observe that $D(\alpha)$ is continuous in $(1-B_2/\lambda\mu, B_1/\lambda\mu)$. Based on constraints (2) and (3), we have $1-B_2/\lambda\mu < 0$ and $B_1/\lambda\mu > 1$. Hence, $D(\alpha)$ is continuous in [0,1]. To find the extreme points, the derivative of $D(\alpha)$ is calculated:

$$D'(\alpha) = \frac{a\alpha^2 + b\alpha + c}{f^2(\alpha)},$$

where

$$\begin{aligned} a &= \lambda^2(B_1 - B_2), \\ b &= 2\lambda B_1(-\lambda\mu + 2B_2)/\mu, \\ c &= B_1(B_2^2 - 2\lambda\mu B_2 + \lambda^2\mu^2 - B_1B_2)/\mu^2, \\ f(\alpha) &= \sqrt{\mu}(-\lambda\alpha + B_1/\mu)(\lambda\alpha + B_2/\mu - \lambda). \end{aligned}$$

Here, $f^2(\alpha) \neq 0$ when $\alpha$ is in [0,1]. Since $a < 0$ and $b^2 - 4ac > 0$, $D'(\alpha)$ has two zero points $\alpha_1$ and $\alpha_2$. We observe that

$$\alpha_1 = \frac{\lambda\mu\sqrt{\beta}/B_2 + \sqrt{\beta}\left(\sqrt{\beta}-1\right)}{\lambda\mu\left(\sqrt{\beta}+1\right)/B_2}, \tag{4}$$

$$\alpha_2 = \frac{\sqrt{\beta}\left[1 - B_2\left(\sqrt{\beta}+1\right)/(\lambda\mu)\right]}{\sqrt{\beta}-1}, \tag{5}$$

$$\alpha_2 - \alpha_1 = \frac{2\sqrt{\beta}[1 - B_2(\beta+1)/(\lambda\mu)]}{\beta - 1}, \tag{6}$$

where $\beta = B_1/B_2$ and $\beta < 1$. In Eq. (4), the numerator is greater than $\lambda\mu/B_2$ and the denominator is less than $\lambda\mu/B_2$. Thus, we prove that $\alpha_1 < 1$. In Eq. (5), the numerator and the denominator are both less than zero. Hence, we also prove that $\alpha_2 > 0$. In Eq. (6), since the numerator and denominator are both less than zero, $\alpha_2$ is greater than $\alpha_1$. According to the above discussion, we can observe that 1) $D'(\alpha) < 0$ when $\alpha < \alpha_1$ or $\alpha > \alpha_2$ and 2) $D'(\alpha) > 0$ when $\alpha_1 < \alpha < \alpha_2$.

Since $\alpha_1 < 1$ and $\alpha_2 > 0$, we consider four cases: 1) $0 < \alpha_1 < 1$ and $0 < \alpha_2 < 1$, 2) $\alpha_1 \le 0$ and $0 < \alpha_2 < 1$, 3) $0 < \alpha_1 < 1$ and $\alpha_2 \le 0$, and 4) $\alpha_1 \le 0$ and $\alpha_2 \le 0$. In cases 1 and 3, $D_{\min}(\alpha) = D(\alpha_1)$. In cases 2 and 4, $D_{\min}(\alpha) = D(0)$ because $D(0) < D(1)$. After substituting $\alpha = 0$ and $\alpha = \alpha_1$ into $D(\alpha)$, we get

$$D(0) = \frac{\mu}{B_2 - \lambda\mu}, \quad D(\alpha_1) = \frac{2\lambda\mu - B_2\left(1-\sqrt{\beta}\right)^2}{\lambda[B_2(\beta+1) - \lambda\mu]}.$$

Note that $D_{\text{min\_non\_agg}} = D(\alpha_1)$ iff $\alpha_1 > 0$. This means that $\frac{B_2}{\lambda\mu}(1-\sqrt{\beta}) < 1$. ∎

## C. Comparison

*Theorem 1*: The aggregated system has a lower minimum average system delay than the nonaggregated system.

*Proof*: Compared to the minimum average system delay of aggregated, $D(0)$ is obviously less than $D_{\text{min\_agg}}$. Since $D(\alpha_1) - D_{\text{min\_agg}} = \frac{1-B_2(1-\sqrt{\beta})^2/(\lambda\mu)}{\lambda[B_2(\beta+1)/(\lambda\mu)-1]}$, and $B_2(1-\sqrt{\beta}/(\lambda\mu) < 1$, $D(\alpha_1)$ is greater than $D_{\text{min\_agg}}$. ∎

Figure 9 represents the simulation results of the delay for the above two systems. The values of $\lambda, \mu, B_1$, and $B_2$ are set as 0.5/s, 80 Mb, 50 Mpbs, and 100 Mbps, respectively. In each plot, we vary one of these four parameters while keeping the other three as the above values. In Fig. 9(a), the minimum average delay of the nonaggregated system only depends on the bandwidth of the VLC channel until the bandwidth of the WiFi channel increases to 36 Mbps. When $B_1 = 50$ Mbsp, the minimum average delay of the aggregated system is around 50% of that of the nonaggregated system. In Fig. 9(b), as the bandwidth of the VLC channel increases, more requests are allocated to the VLC channel in the nonaggregated system.

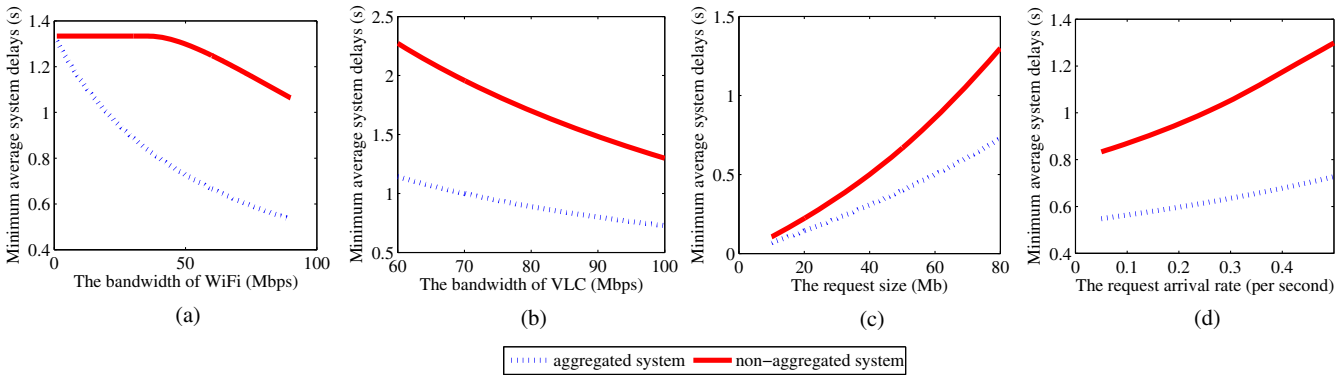


Fig. 9. Minimum average system delays in terms of (a) $B_1$, (b) $B_2$, (c) $\mu$, and (d) $\lambda$.

Therefore, the delay difference between the two systems is decreasing. In Fig. 9(c), we can observe that when the request size becomes extremely small, the delays of the two systems converge to the same value. The reason for this convergence behavior is that reducing the request size will reduce the benefits obtained from splitting the requests in the aggregated system. In Fig. 9(d), increasing the arrival rate has more impact on the minimum average delay of the nonaggregated system than on that of the aggregated system. The analytical results revealed in these four figures also coincide with our theoretical analysis.

This analysis shows how data aggregation can improve system performance, specifically in scenarios in which the WiFi and VLC channels are on the same order of magnitude. It is expected that aggregation will provide diminishing gains over the nonaggregated system as the number of VLC channels increases and the ratio of WiFi capacity to aggregate VLC capacity goes towards 0. This is due to the additional WiFi capacity having a decreasing effect per VLC channel; however, aggregation can provide performance improvements when a small subset of the VLC channels have high traffic demands. This coincides with our results in Section V when considering scenarios in which a single VLC channel uses data aggregation to improve performance for devices associated with it.

## V. Experiments

In this section, we introduce the settings of the experiment testbed and present the throughput and Web page loading time measurement results, to verify the practicability of the VLC-enhanced WiFi system and reveal the benefits of coexisting these two communication techniques. The main experimental parameters are summarized in Table II.

### *A. VLC Front-Ends and Performance of the Single VLC Link*

*1) VLC Front-Ends:* Similar to RF communication, the capabilities of VLC strongly depend on the analog front-ends such as power amplifiers and antennas. Also, the optical source and photodetector have a great effect on the performance of VLC. Our proposed systems, coexisting WiFi and VLC, require high-speed front-ends with PHY and MAC layer implementation. The PC-LED contains a blue light source and is enveloped by a yellow phosphor to produce white light. This low-cost LED provides only narrow modulation bandwidth caused by slow response time of the phosphorescent material. Our collaborators in Fraunhofer-HHI have recently developed a small form

TABLE II
Parameters

| Type of LED | Blue Light With Yellow Phosphor |
|---|---|
| VLC modulation scheme | OFDM |
| Vertical distance measurement range (indoor) | 2–15 m |
| Vertical distance measurement range (outdoor) | 2–10 m |
| Horizontal distance measurement range (indoor) | 0–35 cm |
| Operating system | Ubuntu 12.0.4 LTS |
| Number of users | 1–10 |
| Mode of WiFi router | up to 54 Mbps |
| Bonding driver mode | adaptive load balancing (Mode 6) |
| Throughput measurement runs | over 100 runs |
| Throughput measurement duration | 5 s |
| Web page loading time measurement runs | over 30 runs |
| Blockage duration | 5–30 s |

factor current driver using an off-the-shelf high-power white LED. The VLC receiver consists of a blue filter transimpedance amplifier (TIA) and a commercially available high-speed Si-PIN photodiode (PD). It is reported that the modulation bandwidth has been improved from 3–7 MHz to 20 MHz. This enhancement is realized by reducing the effect of the phosphorescent portion in the optical spectrum with the aid of a blue filter at the receiver end. The new VLC transceiver has significantly increased modulation bandwidth to above 100 MHz by means of precise impedance matching between the LED and the high-power analog driver as well as between the PD and the low-noise amplifier. Fraunhofer-HHI has currently implemented a bidirectional VLC link with a 70 MHz orthogonal frequency-division multiplexing (OFDM) baseband processor. In addition to the VLC front-ends, each device includes a 1 Gbps 802.3 port (wired Ethernet) and external power supply. The use of two modules (transceivers) realizes an Ethernet bridge between two wired end points, allowing the transfer of any IP traffic over the bidirectional VLC link. The performance of the current device yields a gross and net data rate of up to 500 Mbps and 260 Mbps, respectively, with a one-way latency of around 10 ms.

*2) Performance of Indoor and Outdoor VLC Links:* Based on the VLC front-ends developed by our collaborators at Fraunhofer-HHI, we conduct experiments indoors and outdoors to evaluate the average throughput of the VLC link. For the indoor experiment, we measure the throughput within the range of 2–15 m, while the range is 2–10 m for the outdoor experiment. Note that the distance here represents the vertical distance between two transceivers, and the horizontal distance is equal to 0. We also measure the throughput at various horizontal distances within the coverage of the VLC source. All the measurement results are averaged over 100 runs. Each run is a throughput test and spends 5 s. Figure 10 (top) represents the average throughput versus the vertical distance. We achieve around 74 Mbps at 2 m, and the throughput drops to about 25 Mbps at 5 m. Note that the vertical distance for most indoor applications is in this range. Also note that the throughput results here with short vertical distance are higher than the typical throughput that can be achieved by using WiFi with a 2.4 GHz channel conformed to standard 802.11 b/g/n. As we can observe, the throughput results for the outdoor experiment are very similar to those for the indoor experiment. Note that the outdoor environment can represent the extreme condition that happens indoors, with windows open and extensive lighting. The results prove that the VLC front-ends are suitable for the extreme indoor case. Figure 10 (bottom) shows the average throughput when we vary the horizontal distance within the vertical distance from 2 to 5 m.

Note that the data rates measured here are associated with both a customized configuration of the VLC front-ends and a different metric used, compared to [24] and [25]. In particular, different LEDs are used (downlink is white LED, while uplink is infrared, instead of red and blue, respectively). Red LED power is higher in the downlink, and the PD is more sensitive to reddish colors. Due to eye safety, infrared power is more limited in the uplink than for blue

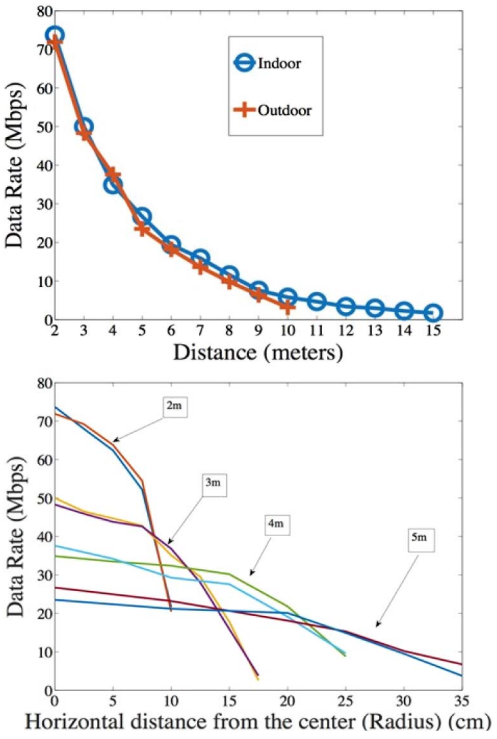


Fig. 10. Throughput versus vertical and horizontal distance between VLC transceivers.

light. Finally, the results in this paper represent the net data rate measured on the application layer in the OSI model, while our previously published data refer to the gross data rate at the physical layer, as it is measured at the baseband processing chipset.

## B. Testbed of the Hybrid System

In the testbed of our proposed hybrid system, we have two PCs with Linux OSs (Ubuntu 12.0.4 LTS), a NETGEAR Wireless Dual Band Gigabit Router WNDR4500, and two VLC transceivers provided by Fraunhofer-HHI. The PC that performs relaying functions is equipped with two Ethernet cards: Intel Corporation 82579LM and 82574L Gigabit Ethernet Controllers. The client PC is equipped with one wireless card and one Ethernet card: a Broadcom 802.11n Network Adapter and a Broadcom NetXtreme Gigabit Ethernet Controller, respectively. All the NICs support 10/100/1000M speed.

Regarding the network configuration, the router's LAN IP address is set to 192.168.1.1/24 as the default. Referring to Fig. 4, the IP addresses of NIC A-1, NIC B-1, NIC A-2, and NIC B-2 are manually configured as 192.168.1.200/24, 192.168.1.100/24, 192.168.2.200/24, and 192.168.2.100/24, respectively. The IPv4 routing table in the client PC is shown in Table III. And an additional entry in the client's ARP table is added by typing "arp -s 192.168.2.1 ab:ab:ab:ab:ab:ab" in the command window with root privilege.

For the VLC unidirectional link setup, since the VLC devices provided by Fraunhofer-HHI are both transceivers,

TABLE III
ROUTING TABLE OF CLIENT

| Destination | Gateway | Genmask | Flags | Metric | Interface |
|---|---|---|---|---|---|
| 0.0.0.0 | 192.168.2.1 | 0.0.0.0 | UG | 0 | eth0 |
| 169.254.0.0 | 0.0.0.0 | 255.255.0.0 | U | 1000 | eth1 |
| 192.168.2.0 | 0.0.0.0 | 255.255.255.0 | U | 2 | eth0 |

we manually turn off the forwarding function in PC I (relay), in order to construct a network-level unidirectional VLC channel. Regarding the VLC connection establishment, there are Ethernet ports on the VLC transceivers; therefore, simply connecting the transceivers to the PCs with Ethernet cable constructs the wireless VLC link.

### C. Testbed of the Aggregated System

To implement the aggregation of two wireless links, we use one PC with Linux OSs (Ubuntu 12.0.4 LTS), a NETGEAR Wireless Dual Band Gigabit Router WNDR4500, a client mode TP-LINK wireless router 150 Mbps TL-WR702N, and also the two VLC transceivers. The client PC is equipped with two Ethernet cards: Intel Corporation 82579LM and 82574L Gigabit Ethernet Controllers. Both the NICs support 10/100/1000M speed. Regarding the network configuration, in order to construct the aggregated system, we add one line to /etc/modules: "bonding mode = 6." After that, we modify the /etc/network/interfaces. We change eth0 and eth1 to auto DHCP and also add the static logic bond0. The detailed commands are shown in Fig. 11.

### D. Results and Analysis

iPerf [26] is a pervasively used tool to measure network performance. Due to the limited bandwidth allocated by the ISP, we set up an internal network with a client, a server, and a router, for the purpose of measuring the achievable bandwidth of the system. We install iPerf on both the client and the server to test the average TCP throughput in all the experiments except the test of Web page loading time. All throughput results are averaged over 100 runs. Each run spends 5 s.

In Fig. 12, we show the average TCP throughput achieved by the three different systems (the two systems described in Section III in addition to a system that uses

```
auto lo
iface lo inet loopback

iface eth0 inet dhcp
iface eth1 inet dhcp

auto bond0
iface bond0 inet static
address 192.168.1.88
netmask 255.255.255.0
gateway 192.168.1.1
up ifenslave bond0 eth0 eth1
down ifenslave -d bond0 eth0 eth1
```

Fig. 11. Bonding configuration.

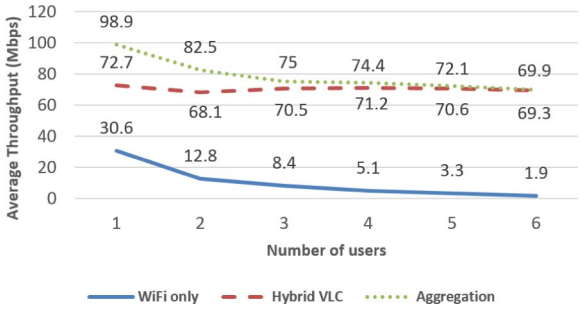


Fig. 12. Throughput versus number of users.

WiFi only). The distance between the transmitter and the receiver is 2 m for both WiFi and VLC. As the number of contending WiFi users is increasing, we test the average TCP throughput obtained by a selected user who uses the three different systems. We set the wireless mode of the router to "up to 54 Mbps"; hence the TCP throughput achieved by the single WiFi user is around 30 Mbps. As the number of users is increasing, the performance of WiFi declines sharply. In contrast, since the contending WiFi users only contend with the uplink wireless channel of hybrid VLC, the throughput of the hybrid VLC user is around 70 Mbps, regardless of the number of users, which is five times higher than the WiFi only users when the number of users increases to six. Also, we can observe that the higher throughput achieved by the aggregated system, which is represented by the dotted line, is almost the aggregated value of the throughput of WiFi only and hybrid VLC. To satisfy the specific users who need extremely high downloading data rates, the aggregated system can be utilized. Note that compared to our previously published work [20], the average throughput is enhanced from 150 kbps (limited by the software-defined VLC) to 70 Mbps [21], which is increased by around 477 times.

In addition to the throughput measurement, we also evaluate the loading time of Web browsing by selecting several representative Web sites. The Pingdom[2] online Web site speed test is used to estimate the loading time of the Web pages. As shown in Fig. 13, we investigate the completion time of the home Web pages of Yahoo, Google, YouTube, and Apple on one client located in a network composed of 10 clients (the other nine WiFi users are downloading a 1 GB file through the same access point). We can observe that the shortest loading time occurs when the selected user chooses the hybrid VLC system. Theoretically speaking, only the WiFi channel could be congested by the other WiFi users; it is reasonable that the loading time of

[2]http://tools.pingdom.com/fpt/.

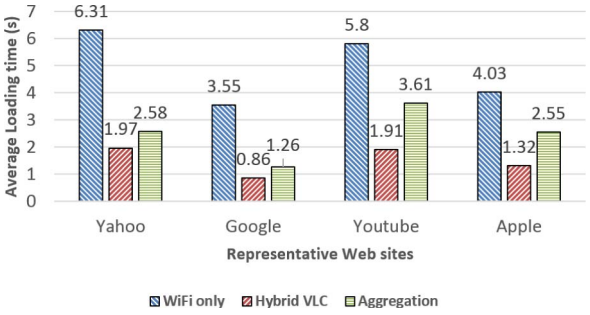


Fig. 13. Loading time in Web browsing.

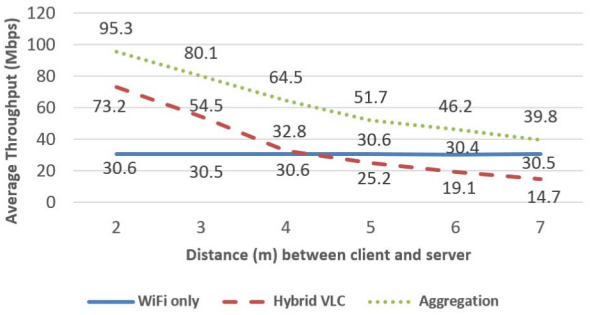


Fig. 15. Throughput versus distance between tx and rx.

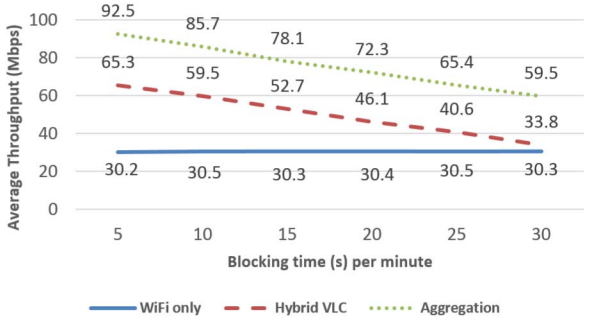


Fig. 16. Throughput versus block duration.

the aggregated system is shorter than the WiFi only but longer than the hybrid VLC. Therefore, based on our implementation, the network performance of the aggregated system is not always better than the hybrid system. This is because the conditions in Section IV are not always satisfied. Our final results of loading time are averaged over 30 runs. Each run is a Web page loading time test via the Pingdom Web site. The statistics of the Yahoo homepage loading time are shown in Fig. 14. Most of the loading times in hybrid and aggregated systems are distributed within the range of 0–5 s. However, three tests' results are distributed in the range of 15–20 s in the WiFi only system. With the WiFi access point congested, the level of network delay may be highly degraded due to the increased back-off penalty.

The short range factor of VLC is inevitable; hence we vary the distance between the transmitter and the receiver for both WiFi and VLC, to measure the average TCP throughput. The experiment results are shown in Fig. 15. As the distance is increasing, the achievable throughput of the hybrid VLC user is decreasing quickly. However, the WiFi only system has stable network performance. The throughput of the WiFi only exceeds the hybrid VLC when the distance is increased to 4.1 m. This is because as the distance increases, the downlink capacity of VLC decreases with distance, eventually becoming insignificant. Note that the throughput results of the hybrid VLC system only depend on the capacity of the VLC downlink. To some extent, the aggregated system is capable of providing a throughput with the lowest bound that is higher than the WiFi only. Therefore, the aggregation technique improves the integrated data rate and offers users more reliable communication.

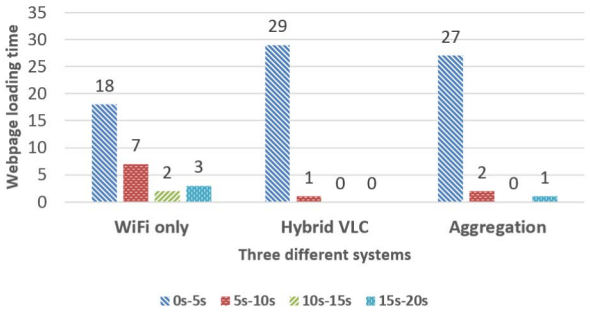


Fig. 14. Statistics of Yahoo homepage loading time.

Due to the particularly small wavelength of the visible light, the VLC channel can be easily blocked by tiny objects. Regarding the irregular movement of mobile devices, the channel blockage duration becomes a considerable factor when we evaluate the network performance of VLC. We vary the blocking time from 5 to 30 s per minute and test the average TCP throughput achieved by the three systems. Figure 16 demonstrates the experiment results. Even if the blocking time in the VLC channel is increased to 30 s per minute, the achievable TCP throughput is still higher than in the WiFi only system. Therefore, compared to the distance, the blocking duration may be less influential. Additionally, although the throughput of the aggregated system is also decreased, it would not be lower than that of the WiFi only system. The blockage duration experiment further proves the robustness of the aggregated system.

## VI. Conclusion and Future Work

In this paper, we evaluate two heterogeneous systems incorporating WiFi and VLC. Our goal is to provide a proof of concept for the coexistence between these two communication bands. Within a short distance between the transmitter and the receiver, the hybrid VLC could perform much better than the WiFi system in the crowded wireless environment. As a complementary technique, VLC deserves further investigation. However, on the one hand,

WiFi infrastructures are prevalent and highly acceptable by most consumers; on the other hand, WiFi may outperform VLC in the case of long-distance data transmission or the existence of obstacles. We have also proven through theoretical analysis that the aggregated system is capable of providing better network performance than that of the nonaggregated system for most delay-sensitive applications. Therefore, we conclude that the aggregation between WiFi and VLC is worthy of further study, to effectively utilize the aggregated bandwidth and to lower the network delay.

For future work, we intend to apply aggregation on the hybrid VLC system. To resolve the challenges of optical uplink in our implemented aggregated system, an approach that integrates the symmetric WiFi only link and the asymmetric hybrid VLC link merits investigation. Another direction for future research is to investigate the issues related to the spatial reuse of VLC links. This requires the utilization of multiple VLC front-ends. Embedding the optimal traffic allocation algorithm into the aggregated WiFi–VLC system and a comparative study between the theoretical analysis and the experimental measurements are also among our future work. Given the benefits and results described in this work, VLC is a promising and evolutionary wireless technology that offers valuable contributions as part of next-generation heterogeneous wireless networks.

## Acknowledgment

This work was supported in part by the NSF grant ECCS-1331018, by the Engineering Research Centers Program of the National Science Foundation under NSF Cooperative agreement no. EEC-0812056, and by the German Ministry of Education and Research (BMBF) through the project OWICELLS under grant no. 16KIS0199K.

## References

[1] "Cisco Visual Networking Index: Forecast and Methodology, 2014–2019," Cisco White Paper, 2015.

[2] M. Kavehrad, "Optical wireless applications: A solution to ease the wireless airwaves spectrum crunch," *Proc. SPIE*, vol. 8645, 86450G, 2013.

[3] J. M. Kahn and J. R. Barry, "Wireless infrared communications," *Proc. IEEE*, vol. 85, no. 2, pp. 265–298, 1997.

[4] T. Komine and M. Nakagawa, "Fundamental analysis for visible-light communication system using LED lights," *IEEE Trans. Consum. Electron.*, vol. 50, no. 1, pp. 100–107, 2004.

[5] S. Rajagopal, R. D. Roberts, and S.-K. Lim, "IEEE 802.15.7 visible light communication: Modulation schemes and dimming support," *IEEE Commun. Mag.*, vol. 50, no. 3, pp. 72–82, 2012.

[6] M. B. Rahaim, A. M. Vegni, and T. D. C. Little, "A hybrid radio frequency and broadcast visible light communication system," in *GLOBECOM*, 2011, pp. 792–796.

[7] C. Lee, C. Tan, H. Wong, and M. Yahya, "Performance evaluation of hybrid VLC using device cost and power over data throughput criteria," *Proc. SPIE*, vol. 8845, 88451A, 2013.

[8] H. Chowdhury, I. Ashraf, and M. Katz, "Energy-efficient connectivity in hybrid radio-optical wireless systems," in *Proc. of the 10th Int. Symp. on Wireless Communication Systems (ISWCS)*, 2013, pp. 1–5.

[9] Z. Huang and Y. Feng, "Design and demonstration of room division multiplexing-based hybrid VLC network," *Chin. Opt. Lett.*, vol. 11, no. 6, 060603, 2013.

[10] S. Schmid, G. Corbellini, S. Mangold, and T. R. Gross, "LED-to-LED visible light communication networks," in *Proc. of the 14th ACM Int. Symp. on Mobile Ad Hoc Networking and Computing*, 2013, pp. 1–10.

[11] K.-D. Langer and J. Grubor, "Recent developments in optical wireless communications using infrared and visible light," in *9th Int. Conf. on Transparent Optical Networks (ICTON)*, 2007, vol. 3, pp. 146–151.

[12] A. L. Ramaboli, O. E. Falowo, and A. H. Chan, "Bandwidth aggregation in heterogeneous wireless networks: A survey of current approaches and issues," *J. Netw. Comput. Appl.*, vol. 35, no. 6, pp. 1674–1690, 2012.

[13] G. P. Koudouridis, R. Agüero, E. Alexandri, J. Choque, K. Dimou, H. Karimi, H. Lederer, J. Sachs, and R. Sigle, "Generic link layer functionality for multi-radio access networks," in *IST Mobile and Wireless Communications Summit*, Dresden, 2005.

[14] G. P. Koudouridis, H. R. Karimi, and K. Dimou, "Switched multi-radio transmission diversity in future access networks," in *2005 IEEE 62nd Vehicular Technology Conf. (VTC)*, Dallas, TX, 2005, pp. 235–239.

[15] A. Yaver and G. P. Koudouridis, "Performance evaluation of multi-radio transmission diversity: QoS support for delay sensitive services," in *IEEE 69th Vehicular Technology Conf. (VTC)*, 2009, pp. 1–5.

[16] J.-O. Kim, T. Ueda, and S. Obana, "MAC-level measurement based traffic distribution over IEEE 802.11 multi-radio networks," *IEEE Trans. Consum. Electron.*, vol. 54, no. 3, pp. 1185–1191, 2008.

[17] J.-O. Kim, "Feedback-based traffic splitting for wireless terminals with multi-radio devices," *IEEE Trans. Consum. Electron.*, vol. 56, no. 2, pp. 476–482, 2010.

[18] J.-O. Kim, P. Davis, T. Ueda, and S. Obana, "Splitting downlink multimedia traffic over WiMax and WiFi heterogeneous links based on airtime-balance," *Wireless Commun. Mobile Comput.*, vol. 12, no. 7, pp. 598–614, 2012.

[19] D. Senie, "Using the SOCK-PACKET mechanism in Linux to gain complete control of an Ethernet interface," 2002 [Online]. Available: http://www.senie.com/dan/technology/sock_packet.html, retrieved Apr. 24, 2002.

[20] S. Shao, A. Khreishah, M. B. Rahaim, H. Elgala, M. Ayyash, T. D. C. Little, and J. Wu, "An indoor hybrid WiFi-VLC Internet access system," in *CARTOON Workshop of CellulAR Traffic Offloading to Opportunistic Networks*, Philadelphia, PA, Oct. 2014.

[21] M. Ayyash, H. Elgala, A. Khreishah, V. Jungnickel, T. Little, S. Shao, M. Rahaim, D. Schulz, J. Hilt, and R. Freund, "Coexistence of WiFi and LiFi towards 5G: Concepts, opportunities, and challenges," submitted to *IEEE Commun. Mag.*

[22] T. Davis, W. Tarreau, C. Gavrilov, C. N. Tindel, J. Girouard, and J. Vosburgh, "Linux Ethernet bonding driver howto," available as download (bonding.txt) from the Linux Channel Bonding project Web site http://sourceforge.net/projects/bonding/ (Nov. 2007).

[23] G. Bianchi, L. Fratta, and M. Oliveri, "Performance evaluation and enhancement of the CSMA/CA MAC protocol for 802.11 wireless LANs," in *7th IEEE Int. Symp. on Personal, Indoor and Mobile Radio Communications (PIMRC)*, 1996, vol. 2, pp. 392–396.

[24] K.-D. Langer, J. Hilt, D. Shulz, F. Lassak, F. Hartlieb, C. Kottke, L. Grobe, V. Jungnickel, and A. Paraskevopoulos, "Rate-adaptive visible light communication at 500 Mb/s arrives at plug and play," *SPIE Newsroom*, Nov. 14, 2013.

[25] L. Grobe, A. Paraskevopoulos, J. Hilt, D. Schulz, F. Lassak, F. Hartlieb, C. Kottke, V. Jungnickel, and K.-D. Langer, "High-speed visible light communication systems," *IEEE Commun. Mag.*, vol. 51, no. 12, pp. 60–66, 2013.

[26] A. Tirumala, F. Qin, J. Dugan, J. Ferguson, and K. Gibbs, "Iperf: The TCP/UDP bandwidth measurement tool," 2005 [Online]. Available: https://lost-contact.mit.edu/afs/atlas.umich.edu/home/PacMan/iperf-1.6.1/doc/.